

Altitude control of a remote-sensing balloon platform

BORGES, Renato Alves <<http://orcid.org/0000-0002-6072-8621>>, BATTISTINI, Simone <<http://orcid.org/0000-0002-0491-0226>>, CAPPELLETTI, Chantal and HONDA, Yago Melo <<http://orcid.org/0000-0002-9094-3584>>

Available from Sheffield Hallam University Research Archive (SHURA) at:

<http://shura.shu.ac.uk/28041/>

This document is the author deposited version. You are advised to consult the publisher's version if you wish to cite from it.

Published version

BORGES, Renato Alves, BATTISTINI, Simone, CAPPELLETTI, Chantal and HONDA, Yago Melo (2021). Altitude control of a remote-sensing balloon platform. *Aerospace Science and Technology*, 110, p. 106500.

Copyright and re-use policy

See <http://shura.shu.ac.uk/information.html>

Altitude control of a remote-sensing balloon platform

Renato Alves Borges^a, Simone Battistini^b, Chantal Cappelletti^c, Yago Melo Honda^a

^a*University of Brasília, Brasília, Brazil*

^b*Sheffield Hallam University, Sheffield, United Kingdom*

^c*University of Nottingham, Nottingham, United Kingdom*

Abstract

This paper addresses the problem of altitude control of stratospheric balloon platforms. Over the last years, there has been an increasing interest in the development of balloon platforms with the ability of maneuvering and fluctuating at the stratosphere for different applications on the basis of remote-sensing. Considering the current trend of a high connected world with sensor grids spread in wide geographical areas, the interest in balloon platform applications has increased posing new challenges for future applications. One of the major problems encountered in this context is how to guarantee constant altitude sustainability. Although the technologies required to address this problem already exist, low cost and easy to launch solutions are still needed considering applications on a wide scale. In this work, a theoretical model of the balloon dynamic is presented and validated. A valve control loop mechanism is proposed for rubber balloons. The controller is tuned empirically and numerical simulations conducted for performance analysis and a case study in a real mission. The proposed solution contributes to increase the capacity of rubber balloons by proposing an altitude control system that allows fluctuation stages which, in general, are not common with this type of balloon.

Keywords: High Altitude Platform, Altitude control, rubber balloon, CubeSat

1. Introduction

2 Nowadays, no one doubts the importance and fundamental role of using
3 scientific balloons floating in the stratosphere. Since the modern era of these

4 lighter-than-air platforms in the early 1930s, characterized by the develop-
5 ment of low density polyethylene films, many different balloon missions were
6 developed, tested, and successfully demonstrated for a variety of applications
7 [1]. For example, from a commercial point of view, balloon platforms provide
8 a way for companies to explore surveillance applications, communication and
9 data services in remote areas, vertical sensing for meteorological applications,
10 and alternatives to conventional rocket launching [2], [3]. From a scientific
11 perspective, they represent a low cost tool for conducting educational ac-
12 tivities [4, 5, 6] or to perform experiments in a near-Earth environment [7].
13 Programs from national space agencies in Europe, USA and Japan, and the
14 recent Google Loon are among some of the efforts to use high altitude bal-
15 loons for data and connectivity services [8], [9].

16 In order to increase the scale and applicability of balloon systems, it is
17 necessary to improve the capability of achieving altitude control, a problem
18 that is currently debated in the literature [10], [11], [12], [13], [14], [15].
19 Different factors contribute to make ballooning systems very challenging,
20 as for instance unknown and constantly changing surface layer winds, high
21 temperature and pressure gradients along the flight path, nonstandard and
22 also changing atmosphere resulting in uncertainties on estimation of height,
23 ascent/descent rate, besides others. Moreover, despite the advances in the
24 mathematical models providing a better description of a balloon flight, most
25 of the data are still unknown to some extent.

26 Future trends in balloon activities are aligned with the current era of high
27 connectivity, internet of things and device to device communication. In this
28 new paradigm, the ability to provide quick response is crucial, and the use
29 of ballooning systems can be of great relevance in supporting activities on
30 ground such as navigation, remote sensing, surveillance and monitoring, spe-
31 cially in remote areas underserved by terrestrial networks or dispersed over
32 a wide geographical area. Lightweight, low-cost platforms that are easy to
33 launch, capable of sustaining its altitude for a period of time, and equipped
34 with a landing control system are among the most suitable solutions to re-
35 spond quickly. This means extending the application of rubber balloons, used
36 mainly for the measurement of meteorological parameters, for more complex
37 missions. Different from zero-pressure and super-pressure balloons, rubber
38 balloons are inexpensive, easy to handle at launch, and safer with respect to
39 flights over densely populated regions due to their lighter weight.

40 It is important to emphasize that rubber balloons have been used primar-
41 ily for meteorological remote sensing since 1920s. They are indispensable for

42 observing weather in the upper atmosphere, as in the case of observations
43 that exploit the reduction in atmosphere influence, or with the observation
44 of the thin atmosphere [16]. It is possible to expand their capabilities to
45 cope with a wider range of applications by adding an exhaust valve that
46 automatically release the lifting gas to control its altitude.

47 Within this context, the Laboratory of Simulation and Control of Aerospace
48 Systems at the University of Brasília, Brazil, has been developing a modular
49 platform able to fluctuate at high altitudes. The platform, called LAICAnSat,
50 is equipped with a system for automatic deployment of small payloads for
51 quick return from the stratosphere. A landing control system enables trajec-
52 tory control in the landing stage, a solution that is very useful for instance
53 to enable easy rescue [17]. The platform is carried to high altitudes using a
54 free-flying, low-cost rubber balloon enabling wide range observations. In its
55 current version, the platform is manufactured in accordance with the Cube-
56 Sat standard [18] using rapid prototype technologies and exploiting current
57 technological advances such as miniaturization of electronic components and
58 devices.

59 Altitude control of a balloon is achieved by either changing the buoyancy
60 of the balloon or its mass. Changing the buoyancy is obtained by changing
61 the volume of the balloon, as done, for example, in [19] by mechanical com-
62 pressing the balloon, or in [20] by heating the gas inside the balloon. Mass
63 alteration requires the capacity of ejecting air (or another kind of ballast)
64 out of the balloon, as done with the Google Loon super pressure balloons
65 [21]. Many methods have been proposed in the literature for the problem of
66 positioning control of high-altitude platforms and airships, such as PID con-
67 trollers [22], backstepping [23], and sliding mode control [24]. On the other
68 hand, very few sources can be found focusing on the design and implemen-
69 tation of altitude control systems for rubber balloons. The altitude control
70 of a rubber balloon presents some peculiar difficulties, indeed. For example,
71 they can not withstand high pressures and the allowed weight is reduced -
72 usually no more than 10 *kg*.

73 This work aims at presenting a simple and practical altitude control sys-
74 tem for the rubber balloon used in LAICAnSat missions. The development
75 of the control system involves the design and manufacturing of a valve for the
76 balloon and a proportional–integral–derivative (PID) controller based archi-
77 tecture, with position and velocity feedback loops. A simple mathematical
78 model of the vertical motion is also developed, which includes some of the
79 most relevant parameters of the balloon, such as the radius and the drag



Figure 1: LAICAnSat-5 and LAICAnSat-5.1 flight models at launching site.

80 coefficient. These parameters are determined in this paper comparing the
81 model with real data collected in previous flights.

82 This paper is organized as follows. Section 2 gives an overview of the
83 LAICAnSat platform and of the main stages of the project so far; Section 3
84 describes the altitude control system; the numerical simulations are reported
85 in Section 4; final conclusions are given in Section 5.

86 2. The LAICAnSat

87 The LAICAnSat project was started in 2013 at the University of Brasilia
88 as an initiative to stimulate the study of aerospace systems and to provide a
89 low-cost platform for hands-on aerospace education. The first flight tests took
90 place in 2014 (LAICAnSat-1 and LAICAnSat-2) [25], [26], and allowed to test
91 early hardware solutions. Other four launches occurred in 2017 (LAICAnSat-
92 3, LAICAnSat-4, LAICAnSat-5 and LAICAnSat-5.1). LAICAnSat-3 and
93 LAICAnSat-4 were launched in order to validate a new mechanical structure
94 fabricated in accordance with the CubeSat standard and using rapid proto-
95 type technologies based on 3D printer manufacturing [27], the new PC/104
96 standard PCB with the on-board computer and embedded sensors [28], as
97 well as two 360° spherical cameras.

98 LAICAnSat-5 (CubeSat 3U standard) and LAICAnSat-5.1 (CubeSat 1U
99 standard), shown in Fig. 1, were launched within the NASA Space Grant
100 Eclipse Ballooning Project [29]. The goal of this mission was to record a
101 360° video reproducing the flight experience up to the stratosphere during

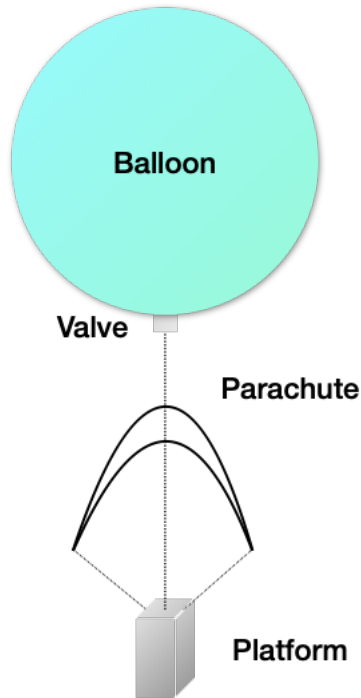


Figure 2: **LAICAnSat system main elements.**

102 the total solar eclipse of August 2017 in North America [30], and a vertical
 103 meteorological mapping of the whole flight path [29].

104 In order to improve the platform, making it more robust and reliable
 105 for more complex missions, a solution capable of performing a completely
 106 autonomous mission, including data collection and safe landing using an
 107 airdropped system was studied in [31]. The use of an airdropped system to
 108 accomplish these tasks is inspired by different types of applications, such as
 109 aerial delivery applications and recovery of payloads from the International
 110 Space Station (ISS), among others.

111 Fig. 2 shows the concept of the LAICAnSat system. The three main
 112 elements are the balloon, the valve, and the platform. A rubber balloon
 113 is used to raise the platform to the stratosphere, where the mission takes
 114 place. The platform is a pseudo-satellite carrying on the payload and all the
 115 subsystems needed for the execution of the mission. A parachute is always
 116 used to safely land the payload in any situation, that is, when released by
 117 using a separating mechanism, or when the balloon suddenly bursts.

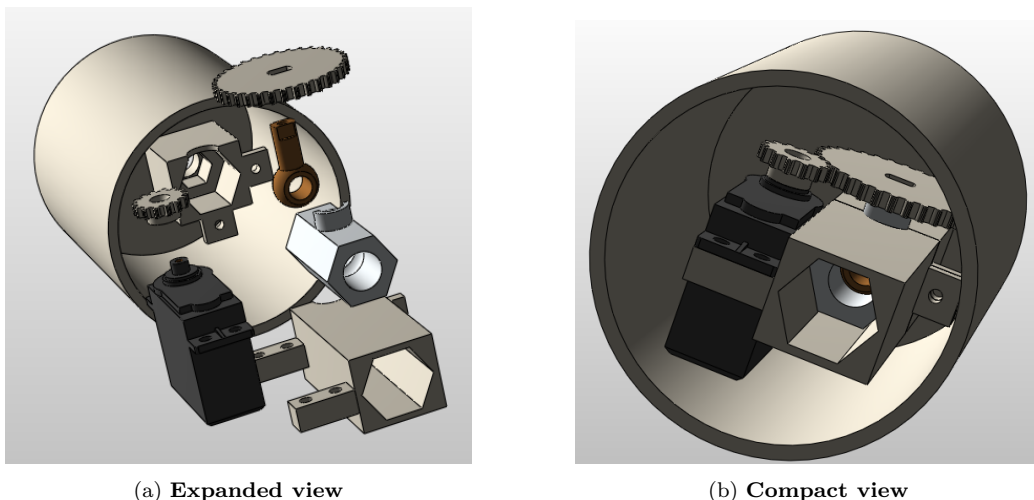


Figure 3: **View of the valve and the actuation system.**

118 *2.1. The balloon*

119 Rubber balloons (sometimes called also meteorological or stratospheric
 120 balloons) are inflatable, rubber-made balloons that can rise up to more than
 121 20 Km in the sky, when filled with a lighter-than-air gas like Helium. They
 122 have great elongation characteristics being able to stretch more than 500%
 123 in one direction. After being partially inflated on the ground, they start to
 124 ascend. The size of these types of balloons is limited by the manufactur-
 125 ing method applied. Different from zero-pressure, super-pressure and dual-
 126 balloons, they are inexpensive and easy to handle when launched. They do
 127 not have a fixed volume, and once their expansion limit is reached at high
 128 altitudes, they burst. Moreover, they are classified by their total mass [16].

129 *2.2. The valve*

130 In order to allow for some fluctuation around a specific altitude, there
 131 must be the possibility to control the amount of internal gas, so that the
 132 internal pressure can be adjusted. This can be done with a valve and a
 133 dedicated strategy for the control of its opening. A valve prototype was
 134 developed, whose main features are low cost, low weight, modularity, and
 135 simplicity of operation.

136 The valve was manufactured with rapid prototyping employing polylactic
 137 acid (PLA). The main component of the project is a commercial-off-the-shelf
 138 (COTS) ball valve, made of copper and zinc. The ball valve was selected

139 taking inspiration from the models used in rocket competitions to control
140 the flow of nitrous oxide for hybrid rockets. The valve has been mechanically
141 coupled to a servomotor and a set of gears to form the actuation system, as
142 shown in Fig. 3. Based on the flight heritage of past tests [31], this system
143 is placed inside the nozzle of the balloon, in order to avoid contacts with the
144 rope that connects the balloon to the rest of the platform.

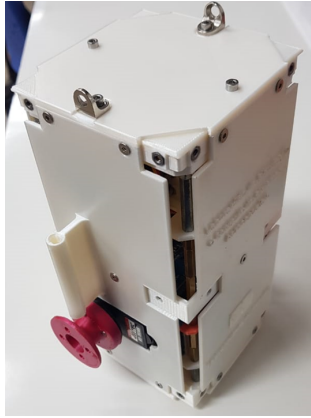
145 To determine the performance of the 1 *cm* diameter ball valve, a leak test
146 was performed using a 0.5 *m* diameter rubber balloon filled with Helium.
147 The valve did not show any noticeable leak for more than 15 minutes. When
148 the valve was opened, the balloon completely deflated in few seconds.

149 *2.3. The platform*

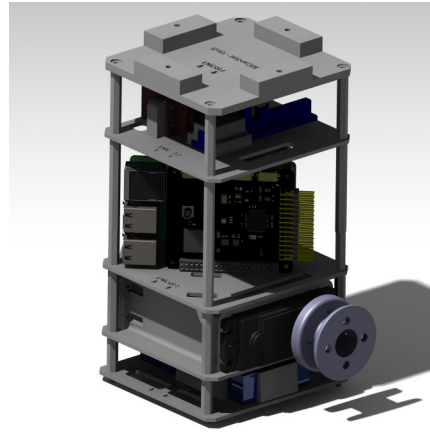
150 The platform of the LAICAnSat is designed following the criteria of
151 the CubeSat standard [18]. The result of this choice is a simple, easy-
152 to-manufacture, and easy-to-access structure. Other advantages of using
153 a CubeSat structure are the possibility to train students in the study and
154 design of aerospace systems and its modularity. The latter allows to develop
155 and internally rearrange the subsystems in accordance to the mission. For
156 example, the payload might change from time to time, but its dimensions
157 will remain defined by the standard.

158 Apart from the first two missions, the platform has been defined as a two
159 (2U) or three-unit (3U) CubeSat. Each unit has dimensions of $10 \times 10 \times 10$
160 *cm* and the internal volume is compatible with the PC/104 standard for em-
161 bedded systems, see Fig. 4. This allows to store the on-board computer, the
162 tracking hardware, batteries, actuators, the payloads and thermal insulation
163 material, if needed. It is important to notice that the final structure might
164 not fully adhere to the CubeSat standard, because of appendages or actua-
165 tors leaning off the walls. For example, a system of servos and pulleys was
166 designed to control the actuation of the parachute, with the actuators and the
167 parachute attachment point being on the external faces of the structure, as
168 shown in Fig. 4a. The platform is manufactured using 3D printing technol-
169 ogy and PLA filaments that provide a robust, lightweight, and UV-resistant
170 structure.

171 The on-board avionics consists of a set of meteorological sensors, a GNSS
172 module, an inertial measurement unit, and a tracking and telemetry xBee-
173 based system working at 900 MHz. The microcontroller is based on a 32
174 bit ARM processor, Cortex-M4, 72 MHz, compatible with Arduino software
175 and libraries [32], [33]. The tracking hardware is a COTS solution that uses



(a) Detail of a LAICAnSat 2U with external servo motors and parachute attachment point.



(b) Internal structure concept of the LAICAnSat 2U.

Figure 4: LAICAnSat current version.

176 the Automatic Position Reporting System (APRS), which is an AX.25-based
177 amateur communication protocol [28]. A redundant tracking system based
178 on a commercial satellite service is also used.

179 The payload changes in accordance with the missions. As remote sensing
180 was among the primary goals in all the missions so far, a number of different
181 cameras were tested throughout the project, namely a GoPro (LAICAnSat-
182 1 and 2), an LG 360CAM and a HackHD 1080p (LAICAnSat-3), a Nikon
183 KeyMission 360 (LAICAnSat-4) and two Kodak Pixpro SP360 4k Virtual
184 Reality (LAICAnSat-5).

185 Lithium Iron Phosphate (LiFePO₄) batteries are used to power the on-
186 board computer due to their light weight and high-energy density. Other
187 devices like the cameras require further batteries (e.g. Lithium-ion ICR)
188 to produce the necessary power. All batteries are fitted inside a box that
189 provides the necessary thermal insulation.

190 3. Altitude control design

191 Altitude control is a very important feature in balloon missions in view
192 of a more complete trajectory control. The flight of a balloon is heavily
193 influenced by the winds, which vary very much according to the altitude [13].
194 Requirements on balloon stabilization are dictated by the remote sensing
195 application and the instruments. For example, in [5] a stable flight of at

196 least 1 *hr* is required for a multi-spectral imaging system mounted on a
 197 balloon. It is important to stress that the main goal of the proposed solution
 198 is to provide a complete mechanism (exhaust valve and control system) to
 199 allow rubber balloon missions to have a fluctuation stage. Moreover, due to
 200 its technical characteristics, missions using rubber balloons are designed to
 201 have a short lifetime. This section will describe the altitude control strategy
 202 designed for the LAICAnSat.

203 3.1. Dynamical model

204 Before designing the altitude control law for the balloon system in this
 205 work, a dynamical model is needed to describe the vertical motion of the bal-
 206 loon. The ascent in the sky of a balloon filled with Helium can be described
 207 by the equilibrium of buoyancy F_B , gravity F_G and aerodynamic F_A forces.
 208 Papers focused on simulating and analyzing balloons flight performance have
 209 considered mass variations resulting from temperature variations in accor-
 210 dance with the standard atmosphere model, solar radiation, and infrared
 211 radiation models [34, 35]. The model used in this work does not include all
 212 these effects, since it is meant at designing a practical control system that
 213 will be compared with real flight data. The equilibrium of forces is, therefore:

$$\dot{v} = \frac{F_B - F_G + F_A}{m}, \quad (1)$$

214 The flat Earth approximation allows to consider gravity as a constant
 215 force directed along the local vertical direction, proportional to the product
 216 of the mass m and the constant gravity acceleration g :

$$F_G = mg \quad (2)$$

217 The buoyancy is given by the difference between the weight of the volume
 218 of gas inside the balloon and the weight of the corresponding volume of air:

$$F_B = V_b(\rho_{atm} - \rho_b)g \quad (3)$$

219 where V_b is the volume of the balloon, ρ_{atm} is the atmospheric density and
 220 ρ_b is the gas density inside the balloon. The aerodynamic force is essentially
 221 the drag force opposed to the motion of the balloon:

$$F_A = \frac{1}{2}C_D\rho_{atm}Sv^2 \quad (4)$$

222 where C_D is the drag coefficient and S is the cross sectional area of the
 223 balloon. The cross sectional area and the volume are not constant, since
 224 the balloon increases its radius r as it rises up in the sky as an effect of the
 225 pressure variation. Initial and burst diameters are provided by the balloon
 226 supplier. The rate of expansion with altitude of the balloon follows a simple
 227 homogeneous dilatation: the balloon geometrical shape is assumed to be a
 228 sphere throughout the whole ascent phase.

229 3.2. Altitude control strategy

230 The altitude control architecture (represented in Fig. 5) is based on
 231 two feedback loops, one on the altitude measurement and the other on the
 232 velocity, alternatively used to open and close the valve of the balloon. Each
 233 control loop is feeding a PID controller that produces an opening command
 234 for the valve, which is implemented by the valve servomotor. The valve
 235 servomotor is modeled as a second order transfer function W_{act} with damping
 236 factor ζ and natural frequency ω_n :

$$W_{act} = \frac{\omega_n^2}{s^2 + 2\zeta\omega_n s + \omega_n^2} \quad (5)$$

237 The altitude control strategy adopted to switch between the two loops
 238 depends on the current mission, flight phase, altitude, and vertical velocity.
 239 It is represented in the flowchart of Fig. 6.

240 The velocity and position reference signals are alternated as references
 241 for the altitude control system, in accordance with the phases of flight. Each
 242 phase, in fact, has a different task with respect to velocity or altitude. The
 243 typical phases of a LAICAnSat mission and their control tasks are defined
 244 as follow:

- 245 1. **Ascent:** The balloon ascends in free flight until reaching a predefined
 246 altitude.
- 247 2. **Altitude control:** Upon reaching the predefined altitude, the control
 248 system is activated acting on the valve. First, the vertical velocity is
 249 reduced to zero. Then, the strategy switches to the position control
 250 loop until it reaches the desired altitude. This floating phase lasts for
 251 the time needed for the system to perform the tasks of the mission.
- 252 3. **Landing:** When the mission is terminated, the velocity loop is acti-
 253 vated once again, making the platform land at a prescribed touch-down
 254 speed.

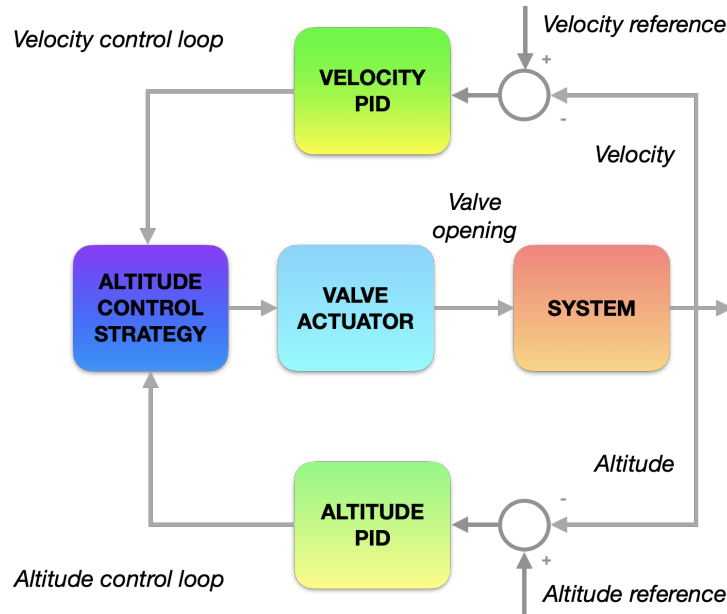


Figure 5: Altitude control architecture

255 **4. Simulations and flight results**

256 In order to validate the dynamic model of Eq. 1 and the control strategy
 257 of Fig. 6, two simulations were performed. The first simulation aims to
 258 reproduce the flight data of the LAICAnSat-5 mission [29], so as to define
 259 values for the parameters of the model in Eq. 2-4. Some of the flight data,
 260 like the temperature, pressure, altitude and vertical velocity profiles, of this
 261 mission are represented in Figs. 7 - 10. The mission reached an apogee of
 262 30 Km in an hour and then touched down in less than another hour. The
 263 second simulation is a representation of an entire mission with the altitude
 264 control strategy described in Section 3.2.

265 The first simulation reproduces the climb and descent of a rubber bal-
 266 loon. In doing so, the unknown parameters of the model are adjusted so to
 267 match the trajectory with that of the LAICAnSat-5 mission. The adjusted
 268 parameters are the drag coefficient C_D and the final radius of the balloon
 269 r_f at burst. For calculating r_f , a linear expansion model has been assumed,
 270 starting from the known initial radius r_0 until finding a suitable value for r_f .
 271 The values of the parameters used in the simulation and the estimated ones
 272 are resumed in Table 1.

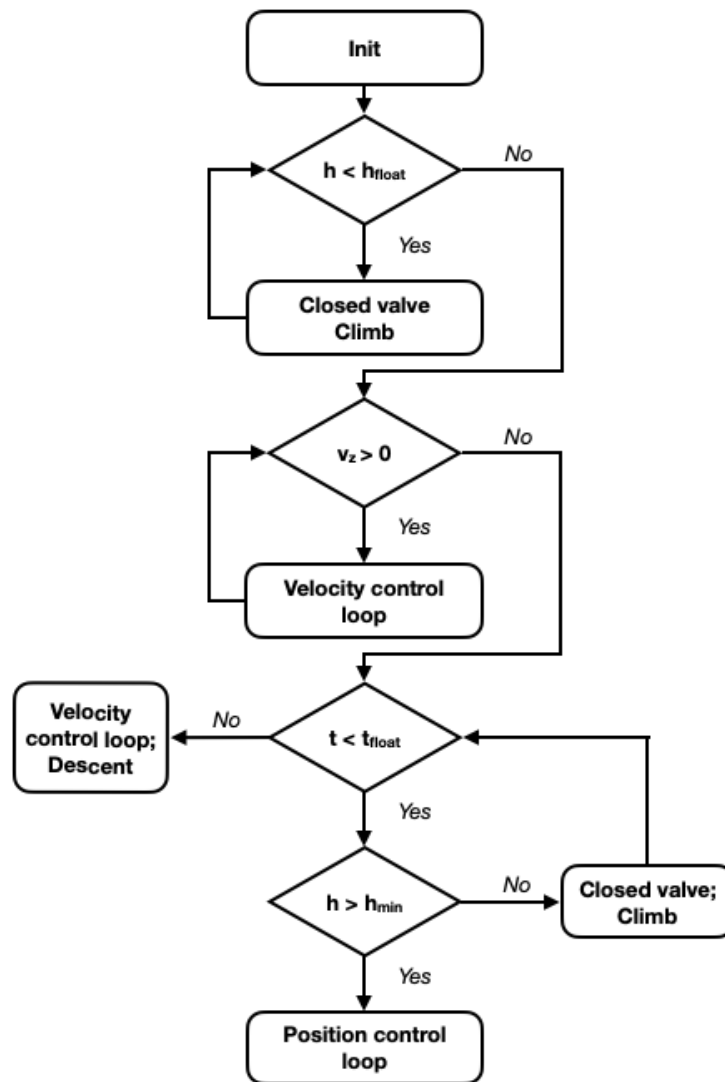


Figure 6: Altitude control strategy

Table 1: **Input variables for the simulation of the dynamic model.**

Parameter	Value	Parameter	Value
g	9.81 m/s^2	C_D	0.85
r_0	1.7 m	r_f	4.65 m
m	4 Kg	Initial Speed	0 m/s
Initial Position	1452 m	Integration Step	0.02 s
ω_n	150 rad/s	ζ	0.7

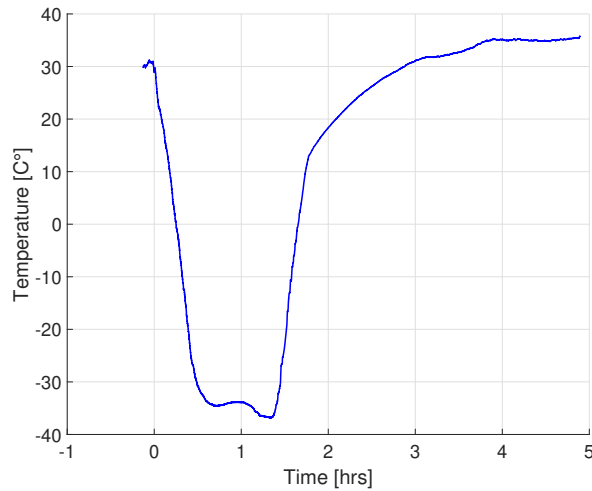


Figure 7: **Temperature profile from the flight data.**

273 Fig. 9 shows the altitude profiles for the LAICAnSat-5 mission and the
 274 simulation. When the balloon reaches the burst altitude observed in the mis-
 275 sion data, the lift force within the simulation is removed and the drag force is
 276 modified to emulate the descent from the platform with a circular parachute.
 277 The two trajectories are quite close, which validates the parameters found for
 278 the dynamic model. Fig. 10 represents the comparison between the vertical
 279 velocity in the simulation and the actual flight data. Even in this case, the
 280 simulated velocity profile is quite close to the recorded data. Flight data
 281 were smoothed using a finite impulse response (FIR) low-pass filter.

282 The second simulation builds upon the model validated in the former
 283 simulation, implementing a complete mission with a fluctuation stage. Fig. 11

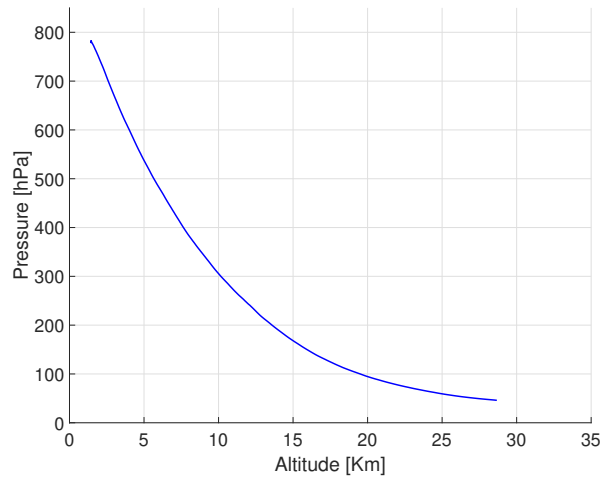


Figure 8: **Pressure profile from the flight data.**

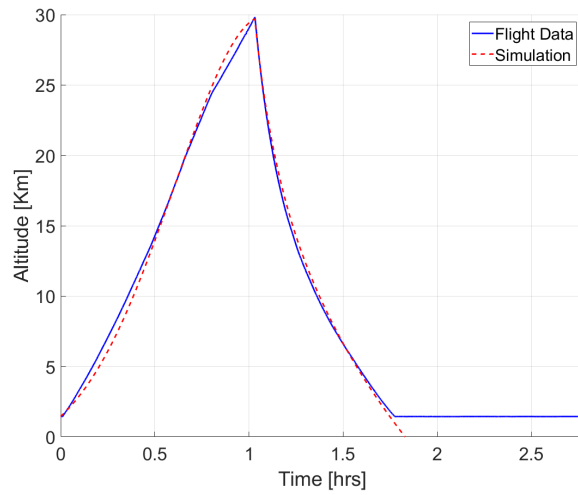


Figure 9: **Altitude profile from the simulation and flight data.**

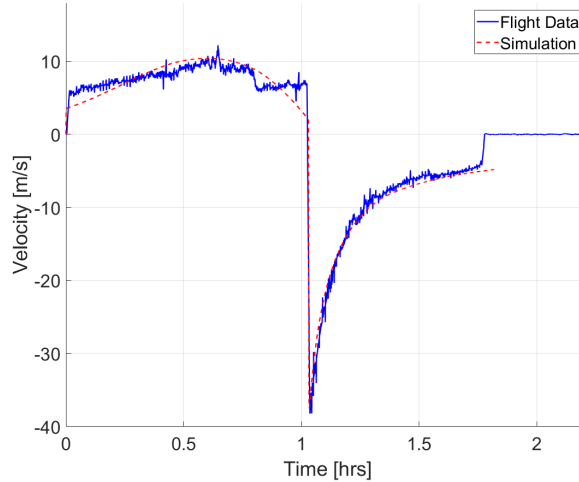


Figure 10: **Vertical velocity profile from the simulation and flight data.**

284 shows the entire altitude profile of a mission taking off at sea level and with
 285 null initial speed. The trajectory has been obtained including in the model
 286 the altitude control strategy described in Section 3.2. The three flight phases
 287 of Section 3.2 have been highlighted to indicate the steps of the mission.

288 Fig. 12 shows the vertical velocity of the system during the simulation.
 289 As expected, it initially grows until the end of the ascent phase and it is then
 290 reduced during the altitude control phase. It can be observed that, after
 291 some chattering in the altitude control phase, the velocity remains at zero,
 292 meaning that the system has reached an equilibrium between the internal and
 293 the external forces. During the landing phase, the velocity becomes negative.
 294 Its absolute value reaches a maximum after 4 hours and then decreases. This
 295 is because gravity acceleration is counteracted by aerodynamic drag, which is
 296 more effective when the speed increases. The drag force allows a reasonably
 297 safe touchdown speed value, around 1 m/s , which is fundamental in order to
 298 preserve the payload.

299 These results show that the proposed control scheme is capable of reg-
 300 ulating the altitude and vertical velocity of the balloon in accordance with
 301 the phases of flight. The flight trajectory of the LAICAnSat-5 mission, in
 302 fact, has been reproduced in simulation while considering practical aspects
 303 as the valve actuator and the physics of the ascent phase. Of course, the full
 304 effectiveness of the control system can be assessed and validated only with

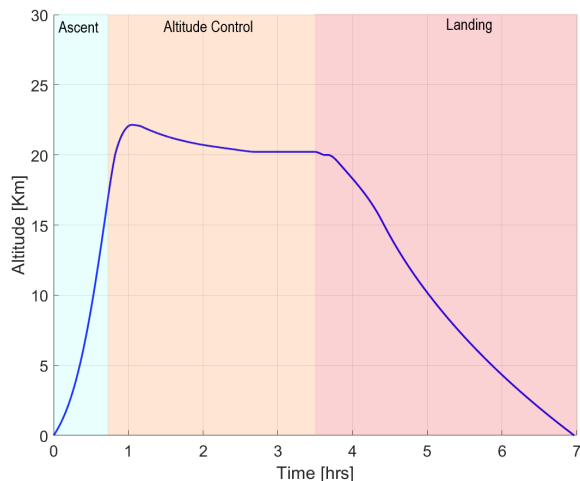


Figure 11: **Altitude profile of the simulated mission with altitude control.**

305 further practical tests. However, the simulation shows that the proposed sys-
 306 tem allows to achieve a substantial floating stage of two hours (see Fig. 12),
 307 during which the vertical velocity is regulated to 0 m/s . This is sufficient to
 308 meet the duration required for the experiment in [5].

309 5. Conclusions

310 In this work, a simple solution for an altitude control system for a rubber
 311 balloon platform is proposed. The design of an actuation system based on a
 312 COTS ball valve for this task has been presented. The actuator is mounted
 313 in an *ad hoc* structure manufactured with rapid prototyping attached to the
 314 balloon nozzle. The proposed approach for the altitude control strategy is
 315 based on the typical phases of a balloon mission. Two PID controllers are
 316 employed for adjusting position and velocity of the platform. The use of two
 317 control loops allows to track the goals of each mission phase. In addition, this
 318 work suggests a simple switching strategy for the PID controllers, and derive
 319 a dynamical model of the vertical motion of the proposed platform. The
 320 parameters of the model are estimated using sample data from a previous
 321 flight of the LAICAnSat system. The results of the simulation show that the
 322 proposed control scheme is able to provide a suitable vertical stabilization.
 323 Future work considers conducting exhaustive flight tests to assess attributes
 324 such as reliability, efficiency, maintainability, among others.

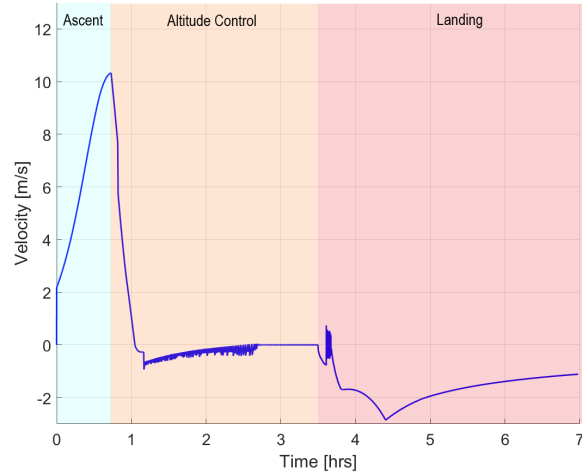


Figure 12: **Altitude profile of the simulated mission with altitude control.**

325 **Acknowledgment**

326 This work is supported by the Brazilian agencies CNPq, FAPDF and
 327 CAPES. The authors would also like to thank Victor Henrique Caldeira
 328 Barbosa for helping with the drawing of the most recent version of the
 329 LAICAnSat platform.

330 **References**

- 331 [1] F. A. d'Oliveira, F. C. L. de Melo, T. C. Devezas, High-Altitude Plat-
 332 forms - Present Situation and Technology Trends, *Journal of Aerospace*
 333 *Technology and Management* 8 (2016) 249–262.
- 334 [2] S. Karapantazis, F. Pavlidou, Broadband communications via high-
 335 altitude platforms: a survey, *IEEE Communications Surveys & Tutorials*
 336 7 (2005) 2–31.
- 337 [3] F. Artigas, I. C. Pechmann, Balloon imagery verification of remotely
 338 sensed phragmites australis expansion in an urban estuary of new jersey,
 339 usa, *Landscape and Urban Planning* 95 (2010) 105–112.
- 340 [4] T. G. Guzik, J. P. Wefel, The high altitude student platform (hasp)
 341 for student-built payloads, *Advances in Space Research* 37 (2006) 2125–
 342 2131.

- 343 [5] J. A. Shaw, P. W. Nugent, N. A. Kaufman, N. J. Pust, D. Mikes,
344 C. Knierim, N. Faulconer, R. M. Larimer, A. C. DesJardins, W. B.
345 Knighton, Multispectral imaging systems on tethered balloons for opti-
346 cal remote sensing education and research, *Journal of Applied Remote*
347 *Sensing* 6 (2012) 063613.
- 348 [6] A. Golkar, Experiential systems engineering education concept using
349 stratospheric balloon missions, *IEEE Systems Journal* 14 (2020) 1558–
350 1567.
- 351 [7] W. V. Jones, Evolution of scientific ballooning and its impact on astro-
352 physics research, *Advances in Space Research* 53 (2014) 1405–1414.
- 353 [8] A. Aragón-Zavala, J. L. Cuevas-Ruíz, J. A. Delgado-Penín, High-
354 altitude platforms for wireless communications, John Wiley & Sons,
355 2008.
- 356 [9] I. Smith Jr, The nasa balloon program: looking to the future, *Advances*
357 *in Space Research* 33 (2004) 1588–1593.
- 358 [10] O. Kayhan, O. Yücel, M. A. Hastaoğlu, Simulation and control of ser-
359 viceable stratospheric balloons traversing a region via transport phenom-
360 ena and PID, *Aerospace Science and Technology* 53 (2016) 232–240.
- 361 [11] S. Saleh, W. He, Ascending performance analysis for high altitude zero
362 pressure balloon, *Advances in Space Research* 59 (2017) 2158–2172.
- 363 [12] R. S. Sudha, J. Ma, K.-M. Lim, H. P. Lee, B. C. Khoo, Numerical evalu-
364 ation of station-keeping strategies for stratospheric balloons, *Aerospace*
365 *Science and Technology* 80 (2018) 288–300.
- 366 [13] H. Du, M. Lv, L. Zhang, W. Zhu, Y. Wu, J. Li, Station-keeping perfor-
367 mance analysis for high altitude balloon with altitude control system,
368 *Aerospace Science and Technology* 92 (2019) 644–652.
- 369 [14] H. Du, M. Lv, L. Zhang, W. Zhu, Y. Wu, J. Li, Energy management
370 strategy design and station-keeping strategy optimization for high alti-
371 tude balloon with altitude control system, *Aerospace Science and Tech-*
372 *nology* 93 (2019) 105342.

- 373 [15] Y. Jianga, M. Lv, W. Zhu, H. Du, L. Zhang, J. Li, A method of 3-D
374 region controlling for scientific balloon long-endurance flight in the real
375 wind, *Aerospace Science and Technology* 97 (2020) 105618.
- 376 [16] N. Yajima, N. Izutsu, T. Imamura, T. Abe, *Scientific Ballooning: Tech-
377 nology and Applications of Exploration Balloons Floating in the Strato-
378 sphere and the Atmosphere of Other Planets*, Springer, 2009.
- 379 [17] O. A. Yakimenko, N. J. Slegers, R. A. Tiaden, Development and testing
380 of the miniature aerial delivery system snowflake, in: *Proceedings of the
381 20th AIAA Aerodynamic Decelerator Systems Technology Conference
382 and Seminar*, AIAA, pp. 1–15.
- 383 [18] A. Mehrparvar, D. Pignatelli, J. Carnahan, R. Munakata, W. Lan,
384 A. Toorian, A. Hutputanasin, S. Lee, *CubeSat Design Specification -
385 Rev. 13*, The CubeSat Program - Cal Poly SLO, 2014.
- 386 [19] P. B. Voss, E. E. Riddle, M. S. Smith, Altitude control of long-duration
387 balloons, *Journal of aircraft* 42 (2005) 478–482.
- 388 [20] R. U. Athar, T. E. Mathews, J. M. Lavigne, K. R. Burns, A. Fry, R. J.
389 Alliss, D. Felton, *Stratospheric c4isr unmanned station (stratacus)*, in:
390 *AIAA Balloon Systems Conference*, p. 3787.
- 391 [21] P. Andurkar, P. Zodpe, A review paper on p roject “loons.”, *Interna-
392 tional Journal of Advanced Research In Computer and Communication
393 Engineering* 5 (2016) 132–138.
- 394 [22] S. van der Zwaan, A. Bernardino, J. Santos-Victor, Vision based sta-
395 tion keeping and docking for an aerial blimp, in: *Proceedings. 2000
396 IEEE/RSJ International Conference on Intelligent Robots and Systems
397 (IROS 2000)(Cat. No. 00CH37113)*, volume 1, IEEE, pp. 614–619.
- 398 [23] J. R. Azinheira, A. Moutinho, E. C. De Paiva, Airship hover stabilization
399 using a backstepping control approach, *Journal of guidance, control, and
400 dynamics* 29 (2006) 903–914.
- 401 [24] Y. Yang, Positioning control for stratospheric satellites subject to dy-
402 namics uncertainty and input constraints, *Aerospace Science and Tech-
403 nology* 86 (2019) 534–541.

- 404 [25] P. H. D. Nehme, R. A. Borges, C. Cappelletti, S. Battistini, Development
405 of a meteorology and remote sensing experimental platform: The
406 LAICAnSat-1, in: 2014 IEEE Aerospace Conference, IEEE, pp. 1–7.
- 407 [26] B. H. A. Noronha, A. V. S. Silva, R. A. Borges, S. Battistini, System
408 identification of a square parachute and payload for the LAICAnSat, in:
409 2015 IEEE Aerospace Conference, IEEE, pp. 1–7.
- 410 [27] M. F. S. Alves, A. P. Wernke, F. C. Pereira, D. H. Gomes, G. S. Lionço,
411 C. H. F. L. Domingos, D. B. d. Trindade, C. Cappelletti, M. N. D. B.
412 Junior, S. Battistini, R. A. Borges, Design of the structure and reentry
413 system for the LAICAnSat-3 platform, in: In proceedings of the 2nd
414 Latin American IAA Cubesat Workshop, IAA.
- 415 [28] R. R. Dias, A. K. de Castro, S. Battistini, R. A. Borges, C. Cappelletti,
416 LAICAnSat-3: A mission for testing a new electronic and electronic
417 and telemetry and tracking system, in: In proceedings of the 2nd Latin
418 American IAA Cubesat Workshop, IAA.
- 419 [29] R. A. Borges, L. T. de M. Corrêa, S. C. Guimarães, A. C. dos Santos,
420 S. Battistini, C. Cappelletti, LAICAnSat-5: A mission for recording the
421 total solar eclipse from the stratosphere, in: Proceedings of the 39th
422 IEEE Aerospace Conference, pp. 1–7.
- 423 [30] A. Des Jardins, S. Mayer-Gawlik, R. Larimer, W. Knighton, J. Fowler,
424 D. Ross, C. Koehler, T. Guzik, D. Granger, J. Flaten, et al., Eclipse bal-
425 looning project live streaming activity: Overview, outcomes, and lessons
426 learned, in: Celebrating the 2017 Great American Eclipse: Lessons
427 Learned from the Path of Totality, volume 516, p. 353.
- 428 [31] V. C. Barbosa, M. N. D. B. Júnior, R. A. Borges, S. Battistini, C. Cap-
429 pelletti, Development of an actuator for an airdropped platform landing
430 system, in: Proceedings of the 41st IEEE Aerospace Conference, pp.
431 1–7.
- 432 [32] M. A. L. Holanda, R. A. Borges, Y. M. Honda, S. Battistini, Trajectory
433 control system for the LAICAnSat-3 mission, in: 2017 IEEE Aerospace
434 Conference, IEEE, pp. 1–7.
- 435 [33] A. C. C. P. de Melo, F. C. Guimaraes, Y. H. M. Honda, R. A. Borges,
436 S. A. P. Haddad, S. Battistini, C. Cappelletti, Design analysis of a

- 437 new on-board computer for the LAICAnSat platform, in: 2019 IEEE
438 Aerospace Conference, IEEE, pp. 1–8.
- 439 [34] Q. Dai, X. Fang, X. Li, L. Tian, Performance simulation of high altitude
440 scientific balloons, *Advances in Space Research* 49 (2012) 1045–1052.
- 441 [35] A. González-Llana, D. González-Bárcena, I. Pérez-Grande, Á. Sanz-
442 Andrés, Selection of extreme environmental conditions, albedo coef-
443 ficient and earth infrared radiation, for polar summer long duration
444 balloon missions, *Acta Astronautica* 148 (2018) 276–284.